CLM - P 282

United Kingdom Atomic Energy Authority

RESEARCH GROUP

Preprint

NUMERICAL SIMULATION OF HYDRODYNAMICS BY THE METHOD OF POINT VORTICES

J P CHRISTIANSEN

Culham Laboratory
Abingdon Berkshire

1971

CLM-P 282

NUMERICAL SIMULATION OF HYDRODYNAMICS BY THE METHOD OF POINT VORTICES

J P Christiansen

(To be submitted for publication in Journal of Computational Physics)

ABSTRACT

The motion of a two-dimensional incompressible inviscid and homogeneous fluid can be described by a Hamiltonian formalism based on the concept of vorticity. A particle model appropriate to this description is presented with a finite difference scheme approximating the equations of motion. The effects of replacing the exact equations by the difference scheme are studied separately. The results from computer simulations employing the scheme on a test model reveal certain undesired features, which are explained by a theoretical analysis in conjunction with various numerical experiments. These experiments have been aimed at understanding the relative importance of each approximation, and also at acquiring a quantitative estimate for possible inaccuracies. It is concluded that the particle model is useful and versatile for a variety of problems in hydrodynamics and plasma physics.

U K A E A Research Group
Culham Laboratory
Abingdon
Berks.

August, 1971

I. INTRODUCTION

Incompressible fluid flows have been the subject of many investigations in plasma physics and hydrodynamics. The nonlinearity of the partial differential equations renders them insolvable except for special cases, but many of the most interesting flow properties must be explained through the nonlinearity. The advent of computers has over the last decade made it a challenging problem to study fluid flows in the nonlinear regime by applying suitable numerical techniques. So far efforts have mainly been concentrated on systems of 1 or 2 dimensions because of computer storage requirements. Many of the numerical approaches to a study of 1- or 2-dimensional hydrodynamic systems work well for continuous flows, but since for many flows discontinuities can be the all-important feature we shall approach the subject with this in mind. This paper describes a useful technique for a numerical attack on nonlinear problems in hydrodynamics, a technique which has also been applied with success in plasma physics.

The motion of a 2-dimensional incompressible, inviscid and homogeneous fluid can be described by a Hamiltonian formalism [1,2] based on the concept of vorticity. This feature makes the system attractive to simulate numerically, especially if one adopts a particle model for the continuous vorticity distribution. The fluid system is in many ways analogous to 1-dimensional systems in plasma physics, gravitational theory, electron beam-plasma systems etc., since these systems exhibit an incompressible flow in 2-dimensional phase space. These analogies emphasise the fundamental character of classical incompressible fluid flow.

A century ago Helmholtz, Kirchoff, Kelvin and others initiated a study of hydrodynamics based on the concept of vorticity, although this quantity had been defined and interpreted by d'Alembert, Euler, Lagrange and Cauchy many years before. (The first treatment of vorticity occurs in the work of d'Alembert (1749)). The initial investigations were concerned with simple vorticity systems; usually uniform vorticity distributions were studied. Despite their simplicity such systems exhibit a great deal of the dynamics

contained within the subject. It is noteworthy that the same simplifications have been made in the study of the analogous 1-dimensional plasma systems during the last decade. The model used in both cases has been called the 'Waterbag Model', since the studies extend to the contours confining uniform distributions.

It is of great interest to study even simple flow configurations in a 2-dimensional phase space to acquire a fundamental understanding of the dynamics of nonlinear flows. In Figs.7 & 8 at the end of this paper we show 7 examples of hydrodynamic systems to emphasize the complexity of nonlinear processes. These 7 systems have been simulated using the numerical techniques discussed in this paper.

To interpret the phenomena that we discover from numerical simulations it is however necessary to understand in detail the effects of replacing the partial differential equations by finite difference forms. These effects can most easily be determined by comparing the numerical solutions of simple well-known problems with their analytic counterparts. Any anomalies such as numerical viscosity which are contained within the numerical scheme will then appear.

In this paper we shall compare the exact Hamiltonian formalism with its equivalent difference form. To illuminate the differences between them we present results from numerical experiments on a test model. In choosing a test model we have found it useful to eliminate the time dependence by studying steady-state equilibrium flows. Any time variations in the numerical simulation then result from anomalous characteristics of the difference scheme. Finally, by a trial and error method we shall detect the sources of the anomalies disclosed by the numerical experiments.

II. EQUATIONS OF MOTION

A 2-dimensional incompressible, inviscid homogeneous fluid (ideal fluid) satisfies the continuity and Navier-Stokes equations

$$\nabla . \underline{u} = 0 \tag{1}$$

$$\frac{\partial \underline{u}}{\partial t} + \underline{u} . \nabla \underline{u} = - \frac{1}{\rho} \nabla P \tag{2}$$

where $\underline{u}$, ρ and P denote fluid velocity, density and pressure respectively. We introduce the vorticity $\underline{f}$ and the stream function $\underline{H}$ by the vector relations

$$\underline{f} = \nabla \times \underline{u} \quad , \quad \underline{u} = \nabla \times \underline{H} \ , \tag{3}$$

the notation being chosen to emphasize the analogy with Vlasov's equation in particle dynamics.

Since $\underline{f} = (o,o,f)$ and $\underline{H} = (o,o,H)$ we can consider $\underline{f}$ and $\underline{H}$ as scalars. If we take the curl of (2) the equation of motion becomes the d'Alembert-Euler vorticity equation

$$\frac{\partial f}{\partial t} + [f,H] = 0 \tag{4}$$

with f and H related by

$$\nabla^2 H = - f \tag{5}$$

(For any two functions A and B the Poisson bracket is defined by $[A,B] = \frac{\partial A}{\partial q}\frac{\partial B}{\partial p} - \frac{\partial B}{\partial q}\frac{\partial A}{\partial p}$) .

The system is Hamiltonian, since by (3)

$$\dot{q} = \frac{\partial H}{\partial p} \qquad \dot{p} = - \frac{\partial H}{\partial q} \quad , \tag{6}$$

where the position vector $\underline{r}$ is $\underline{r} = (q,p)$.

The well-known stream function therefore behaves as a Hamiltonian, and real space acts as phase space. Because of analogies with 1-dimensional systems mentioned earlier we find this notation appropriate and it will be used throughout this paper to emphasize the structure of the equations. Equations (4) and (5) are just Liouville's and Poisson's equations respectively. The invariants of the motion are

Linear momentum $$\underline{P} = \rho \iint_A \underline{u}\, dqdp \tag{7}$$

Angular momentum $$\underline{L} = \rho \iint_A (\underline{r} - \underline{r}_c) \times \underline{u}\, dqdp \tag{8}$$

Kinetic energy $$E = \tfrac{1}{2}\rho \iint_A |\underline{u}|^2 dqdp = \tfrac{1}{2}\rho \iint_A fH dqdp \tag{9}$$

Area elements $$A(f)\, df \quad , \tag{10}$$

where $A(f)df$ is the area of fluid between two vorticity contours $f, f+df$, which by Helmholtz theorem remain attached to the fluid throughout the motion. The Hamiltonian is invariant to translation and rotation in the phase plane (unlike the corresponding Hamiltonian in particle dynamics). The total energy of the system is purely kinetic and the second integral of (9) is correct if

$$\oint_C H \frac{\partial H}{\partial n}\, ds = 0 \quad , \tag{11}$$

where C is a contour bounding the region A.

Any state of this system is entirely described by the vorticity distribution f, which also behaves as a phase-space density distribution. Any part of the fluid with a particular value of f behaves like an incompressible 'vortex fluid'. For equilibrium steady-state flows we have, just as in the analogous case of a plasma

$$\frac{\partial}{\partial t} = 0 \ , \text{ or } [f,H] = 0, \text{ or } f = f(H) \ . \tag{12}$$

III. A PARTICLE APPROACH

There is a variety of ways in which one can develop computational techniques for studying this fluid system. The two functions $f(q,p,t)$ and $H(q,p,t)$ can be represented on a discrete mesh as in the method of Fromm and Harlow [3]. Another technique is to calculate the motion of a limited number of point vortices, interacting with each other via their individual 2-body velocity potentials. This was done by Abernathy and Kronauer [4] in their study of the formation of a von Karman vortex street. A third possibility is to follow the motion of contours f=constant. This has been done successfully in plasma physics for the analogous case of the 1-dimensional Vlasov equation by Roberts and Berk [5] who used the waterbag model earlier adopted by de Packh [6] and Dory [7].

The method used by Christiansen and Roberts [8] is more analogous to the particle methods used in plasma physics. It approximates f by a large number of "point vortices"

$$f = \sum_{n=1}^{N} f_n \, \delta(q - q_n) \, \delta(p - p_n) \tag{13}$$

where $f_n = +1$ or -1. Each pair of coordinates (q_n, p_n) is called a point vortex and satisfies the equations of motion

$$\dot{q}_n = \frac{\partial H}{\partial p_n} \qquad \dot{p}_n = - \frac{\partial H}{\partial q_n} \ , \tag{14}$$

where H is a solution of Poisson's equation (5)

$$H = \frac{1}{2\pi} \sum_{\substack{n=1 \\ n \neq m}} \sum_{m=1} f_n f_m \log r_{nm} \tag{15}$$

with

$$r_{nm}^2 = | \underline{r}_n - \underline{r}_m |^2 \tag{16}$$

excluding the infinite self energy.

Particle models have primarily been used to simulate plasmas. Groups at Livermore, Los Alamos, Stanford and Princeton have developed a variety of numerical techniques and calculations have been reported by Birdsall, Fuss, Byers, Morse, Hockney and Dawson. The techniques discussed in this paper have been used by Taylor and McNamara to study 2-dimensional guiding centre plasma problems [10] which are formally identical to those of an ideal fluid. The diochotron type instability illustrated in Fig.7 was studied by Birdsall and Fuss, whilst the Kelvin-Helmholtz type instability was investigated independently by Byers and Hockney. These authors included a finite Larmor radius, but despite this and other differences in the models used our results agree qualitatively with theirs.

This paper discusses the implications of applying finite difference methods to hydrodynamic problems. Such a study has been made before but usually in connection with plasma problems. Notably the effects of employing the NGP and CIC interpolations have received attention from Birdsall and Fuss [17], Morse [15], Hockney [18] and more recently Langdon [19]. It should, however, be emphasized that the present investigations differ from previous ones. In our case the particle model represents a true continuum, rather than a physical assembly of particles.

IV. A NUMERICAL SCHEME FOR THE MOTION OF POINT VORTICES

Suppose we are given N sets of coordinates (q_n, p_n) on a Cartesian mesh of size N_q by N_p. To evaluate f as given by (13) we use the CIC-method [15] and approximate f at a mesh point (i,j) by

$$f(i, j) = \sum_{n=1}^{N} A_n \Theta\,(i + 1 - q_n, j + 1 - p_n)\,\Theta\,(q_n - i, p_n - j) \qquad (17)$$

where $\Theta(x,y)$ denotes the Heaviside function. The evaluation of A_n is shown below. Poisson's equation (5) can then be solved using the usual 5-point approximation

$$\frac{H(i,j+1) + H(i,j-1) - 2H(i,j)}{(\Delta p)^2} + \frac{H(i+1,j) + H(i-1,j) - 2H(i,j)}{(\Delta q)^2} = -f(i,j) \qquad (18)$$

where Δq, Δp are the mesh spacings. Eq.18 is solved by the Hockney method [14] allowing for a variety of boundary conditions. The velocity field

evaluated at a meshpoint (i,j) is

$$u_q(i,j) = \frac{H(i,j+1) - H(i,j-1)}{2\Delta p}; \quad u_p(i,j) = -\frac{H(i+1,j) - H(i-1,j)}{2\Delta q} \quad . \tag{19}$$

To advance the set of positions (q_n,p_n) one timestep a leapfrog scheme is used. Two sets of coordinates $(q_n,p_n)_{even}$ and $(q_n,p_n)_{odd}$ are introduced expressing the coordinates at alternate times $2s\Delta t$ and $(2s+1)\Delta t$. The equations

$$\dot{q}_n = u_q \qquad \dot{p}_n = u_p$$

then become, letting superscript s denote the time $s\Delta t$

$$\begin{aligned} q_n^{s+1} &= q_n^{s-1} + u_q^s\,(q_n^s,\, p_n^s)\; 2\Delta t \\ p_n^{s+1} &= p_n^{s-1} + u_p^s\,(q_n^s,\, p_n^s)\; 2\Delta t \quad . \end{aligned} \tag{20}$$

The set of coordinates $(q_n^s,\, p_n^s)$ determines the velocity field (also f^s, H^s) which is used to move the other set. Suppose $i \leqslant q_n^s \leqslant i+1$ and $j \leqslant p_n^s \leqslant j+1$ and let $\delta q = q_n^s - i$, $\delta p = p_n^s - j$. The velocity used in (20)is evaluated as

$$\begin{aligned} u(q_n^s,\, p_n^s) = {} & (1-\delta q)(1-\delta p)\; u(i,j) + \delta q(1-\delta p)\; u(i+1,j) \\ & (1-\delta q)\delta p\; u(i,j+1) + \delta q \delta p\; u(i+1,j+1) \quad . \end{aligned} \tag{21}$$

The 4 coefficients represent 4 areas A_n that are also used to evaluate f such that (21) is consistent with (17).

V. THE COMPUTER CODE

The computer code VORTEX [8] solves Eqs. (17)-(21) on a square mesh with $N_p = N_q = 64$, $\Delta q = \Delta p = 1$. Part of the code is the Hockney-Poisson solver POT1 [14] which allows 9 different sets of boundary conditions in q, p. Amongst the more prominent features is the vector integration technique described by Boris and Roberts in an earlier paper [9].

The VORTEX code has also been used extensively to study the diffusion in a two-dimensional plasma using the guiding centre model. This work has been reported by Taylor and McNamara [10].

VI. THE EFFECTS OF THE FINITE DIFFERENCE FORMULATION

Our numerical approach described in sections III to V is an approximation to Eqs.(4) and (5). This approximation is principally limited by

1. The square-shaped boundary
2. The time integration (Δt finite)
3. The mesh (square mesh, Δq, Δp finite)

In the following we will briefly establish the general effects introduced by these limitations and then later apply them to a particular numerical experiment.

VII. THE SQUARE-SHAPED BOUNDARY

Imagine that our simulation problem is that of following the motion of a number of contours enclosing areas of constant $f = f_o$. Initially our distribution function is described by a set of contours expressed by functions

$$G_j(q,p) = 0.$$

The solution to Laplace's equation in a suitable coordinate system is ($\sim$ denotes value outside any contour j)

$$\tilde{H} = \tilde{H}(q,p) \tag{22}$$

where $\frac{\partial}{\partial \underline{r}}(\tilde{H}) \to 0$ (say) for $|\underline{r}(q,p)| \to \infty$. The solution $\tilde{H}$ of Laplace's equation satisfies the set of conditions

$$\tilde{H}(G_j = 0) = H(G_j = 0)$$

where H is a solution of (5).

We then introduce a square boundary and require that $\tilde{H} = H_1$, a constant, along this square G_o. The solution (22) can be expanded in the normal way

$$\tilde{H} = \sum_{n=o}^{\infty} \tilde{H}_n \tag{23}$$

with

$$\tilde{H}_o = \frac{-1}{4\pi} \log r \int_A f(q,p)da = \frac{-1}{4\pi}(\log r)\, f_o \sum A_j + H_c$$

where r is the distance from the origin to the variable point P and

A_j is the area enclosed by contour j. A_j is positive if $f = f_o$ and negative if $f = -f_o$. In general the nth term of the expansion (23) is

$$\tilde{H}_n = \frac{(n-1)!(-1)}{r^{n+1}} \left\{\nabla^n \underline{r}\right\} \cdot \left\{D^{(n)}\right\}$$

where the bracketed quantities are tensors of rank n. If $\sum_j A_j \neq 0$, $\tilde{H}_o$ will normally be the dominant term for sufficiently large r values. This means that, regardless of the choice of coordinate system, $\tilde{H}$ exhibits rotational symmetry. The contour G_o is hence approximately a circle and for convenience we replace the Hamiltonian variables (q,p) by (r,θ) in this section only. The introduction of a square boundary can then be interpreted as a superposition of four images of the set of contours. The images further away are neglected. The resulting potential can be calculated as a superposition of 5 potentials arising from the actual system of contours (k=o) and four image systems (k = 1,2,3,4) placed symmetrically with respect to each of the four boundaries.

If we look at distances r inside the square but far from any contour the dominant term in the expansions (23) is $\tilde{H}_o$. This gives

$$\tilde{H}_o = \sum_{k=0}^{4} \alpha \frac{1}{4\pi} f_o \left(\sum_j A_j\right) \log r_k$$

where $\alpha = -1$ for $k = 0$ otherwise $\alpha = +1$. Inserting r_k as $r_k^2 = r^2 + 4L^2 - 4Lr \cos(\theta + \phi)$, $\phi = 0, -\frac{\pi}{2}, \pi, \frac{\pi}{2}$ for $k = 1,2,3,4$ we get when expanding the log term

$$\tilde{H}_o = -K \log r + K \sum_{m=1}^{\infty} \frac{1}{2m} \left(\frac{r}{2L}\right)^{4m} \cos(4m\theta) \qquad (24)$$

with

$$K = \frac{1}{4\pi} f_o \sum_j A_j \ .$$

Eq.24 shows that rotational modes m=4,8,12 .... have been imposed on the original solution.

For higher order terms in the expansion (23) we find that

$$\tilde{H}_n = \beta_o^{(n)} \frac{1}{r^n} + \sum_{m=1} \beta_{4m}^{(n)} (\cos 4m\theta) \left(\frac{r}{2L}\right)^{4m}$$

where coefficients $\beta_{4m}^{(n)}$ as function of $\cos(4m\theta)$ arise from the expansion of $\frac{1}{r_k^n}$. For n=1 $\beta_{4m}^{(1)}$ become the Legendre polynomials.

In order to evaluate the effect of introducing a square boundary we see that first we must estimate the relative weight of the terms $\tilde{H}_n$ for $n=0,1,2 \ldots$

Once this is done we must evaluate the coefficients for $m=4,8,12$ modes in the expansion of $\tilde{H}_n$ and compare their amplitudes with the log r term. The maximum effect on the distribution of vorticity will occur when the coefficients are evaluated at the largest r for which $f \neq 0$.

VIII. THE EFFECT OF A FINITE TIME INTEGRATION

We are primarily interested in the stability of the finite time integration implemented by the leapfrog scheme. To examine this assume that we move two independent sets e and o of points. We assume for simplicity that the points move in a time independent velocity field so that H is constant in time. As a result of applying finite Δt to the motion of the points e and o we imagine that the limit $\Delta t \to 0$ results in a symmetrical displacement around the correct value $\underline{R}_c$

$$\underline{r}_e(t) = \underline{R}_c + \underline{\delta}, \quad \underline{r}_o(t) = \underline{R}_c - \underline{\delta} \quad .$$

Inserting for $\underline{r}_e$ and $\underline{r}_o$ in $\frac{d\underline{r}}{dt} = \underline{u}$ and subtracting we get

$$\frac{d\underline{\delta}}{dt} = - \frac{d\underline{u}}{d\underline{r}} \underline{\delta} \quad . \tag{25}$$

Suppose $\underline{\delta} = (\delta_q \hat{\underline{q}} + \delta_p \hat{\underline{p}}) \, e^{ist}$ where both δ_q, δ_p may be functions of q, p and $\hat{q}$ and $\hat{p}$ are the base unit vectors of an orthogonal coordinate system. To find whether s can become complex we insert for δ in Eq. 25

$$\frac{d}{dt} (\delta_q \hat{\underline{q}}) + \frac{d}{dt} (\delta_p \hat{\underline{p}}) + is (\delta_q \hat{\underline{q}} + \delta_p \hat{\underline{p}}) + \delta_q \nabla u_q + \delta_p \nabla u_p = 0 \quad . \tag{26}$$

Eq.26 will express the eigenvalues λ of s as $g(\underline{\delta}) = \lambda \delta$, through a quadratic equation in s which, since $\nabla . \underline{u} = 0$ becomes

$$-s^2 + S (u_q, u_p) = 0 \quad .$$

The condition for stability is then

$$S (u_q, u_p) \geqslant 0 \quad .$$

In cartesian coordinates $(q,p) = (x,y)$ we get

$$\frac{\partial u_x}{\partial x}\frac{\partial u_y}{\partial y} - \frac{\partial u_x}{\partial y}\frac{\partial u_y}{\partial x} \geqslant 0 \quad .$$

In polar coordinates $(q,p) = (\tfrac{1}{2}r^2, \theta)$ we get

$$\tfrac{1}{2}\frac{1}{r}\frac{\partial(u_r^2 + u_\theta^2)}{\partial r} + \frac{1}{r}\frac{\partial u_r}{\partial r}\frac{\partial u_\theta}{\partial \theta} - \frac{1}{r}\frac{\partial u_r}{\partial \theta}\frac{\partial u_\theta}{\partial r} \geqslant 0 \quad . \tag{27}$$

We notice that for a simple steady state flow described by $\underline{u} = \underline{\omega}(r) \times \underline{r}$ with $u_r = 0$ $u_\theta = \omega(r)r$ Eq.27 becomes

$$\omega^2(r)\left[1 + r\frac{d\ln\omega(r)}{dr}\right] \geqslant 0.$$

from which we deduce that the leapfrog scheme causes the frequently encountered irrotational flow $\omega \sim r^{-2}$ to become unstable. The implications of this result will be dealt with in the description of the test model.

IX. EFFECTS INTRODUCED BY THE MESH

In IV we have presented the finite difference forms used to approximate Eqs. (4) and (5).

Let us look at each difference form separately to see how good an approximation it is. Throughout this section we will consider functions represented by a finite series of harmonics. For simplicity we choose

$$\cos rq \quad \cos sp$$

with $r = \frac{\pi\ell}{N_q}$ or $\frac{2\pi\ell}{N_q}$ and $s = \frac{\pi k}{N_p}$ or $\frac{2\pi k}{N_p}$ depending on which type of boundary condition is imposed on the functions.

a) Poisson's equation

Consider a mesh function represented correctly at all meshpoints as

$$f = \sum_\ell \sum_k \cos rq \cos sp \quad . \tag{28}$$

The analytic solution to Eq.(5) using (28) is for a particular mode r,q

$$H = \left[r^{-2} + s^{-2}\right]\left[\cos rq \cos sp\right] \quad . \tag{29}$$

Insertion of Eq.(29) in (18) setting $r^{-2} + s^{-2} = K$ gives us f_Δ. We form the ratio $\frac{f_\Delta}{f}$ and get the expression

$$\frac{f_\Delta}{f} = K \left[2 \cos r + 2 \cos s - 4 \right] . \qquad (30)$$

b) Evaluation of fluid velocity

Similarly for Eq.(19) we can assume that say $u_q = \cos rq \cos sp$ with the solution (analytic)

$$H = \frac{1}{s} \cos rq \sin sp \qquad (31)$$

Inserting Eq.(31) in Eq.(19) we get

$$u_q^\Delta = \frac{1}{s} \cos rq \sin sp \sin s \qquad (32)$$

such that $\frac{u_q^\Delta}{u_q} = \frac{1}{s} \sin s \approx 1$ when p is small

Exactly the same relation holds for $\frac{u_p^\Delta}{u_p}$ with q inserted for p on the righthand side.

To get an idea of the truncation of harmonics caused by the difference forms (18,19) we can assume that we are given

$$f = 2 \frac{s}{r^2+s^2} \cos rq \cos sp$$

which results in a velocity u_q

$$u_q = - \cos rq \sin sp .$$

Combining Eqns.(30 and (32) gives

$$u_q^\Delta = \eta_q \cos rq \sin sp$$

where

$$\eta_q = \frac{\sin s}{s} \frac{r^2 + s^2}{2(\cos r + \cos s - 2)}$$

and similarly

$$\eta_p = \frac{\sin r}{r} \frac{r^2 + s^2}{2(\cos r + \cos s - 2)} .$$

Set $r = \frac{\pi \ell}{64}$ and $s = \frac{\pi k}{64}$ (VORTEX) and let us see how many modes are subject to a truncation less than 5%, i.e. $\eta \gtrsim 0.95$. A rough estimate gives $\ell = k = 16$.

c) Area weighting of velocities

The approximation (21) finds an interpolated velocity (u_q, u_p) at the position (q_n^s, p_n^s) by what is known as the CIC method [15,17]. To find the effect of this interpolation we assume that u_q is correctly given at all meshpoints as

$$u_q = \cos rq \cos sp \quad .$$

Setting the positions inside the box to δq, δp then the analytically correct velocity at $q_o + \delta q$, $p_o + \delta p$ is

$$u_q = \cos r\,(q_o + \delta q) \cos s\,(p_o + \delta p) \quad . \tag{33}$$

The velocity found by Eq.(21) is

$$u_q^\Delta = A_1\cos(rq)\cos(sp) + A_2\cos(rq+r)\cos(sp) + A_3\cos(rq)\cos(sp+s) + A_4\cos(rq+r)\cos(sp+s) \quad , \tag{34}$$

where superscript Δ denotes the finite difference form.

To find the net difference between u_q and u_q^Δ we perform a Taylor expansion of u_q at the point (q_o, p_o).

$$u_q(q+\delta q, p+\delta p) = u_q(q,p) + \frac{\partial u_q}{\partial q}\,\delta q + \frac{\partial u_q}{\partial p} + \delta p + \tfrac{1}{2}\left(\frac{\partial^2 u_q}{\partial q^2}\,\delta q^2 + \frac{\partial^2 u_q}{\partial p^2}\,\delta p^2 + 2\,\frac{\partial^2 u_q}{\partial q \partial p}\,\delta q \delta p\right) \tag{35}$$

The form u^Δ can similarly be written in terms of the finite difference forms of the derivatives

$$u_q^\Delta(q+\delta q, p+\delta p) = u_q(q,p) + \left[\frac{\partial u_q}{\partial p}^{\Delta}\right]_{\frac{1}{2},o}\delta q + \left[\frac{\partial u_q}{\partial p}^{\Delta}\right]_{o,\frac{1}{2}}\delta p + \left[\frac{\partial^2 u_q}{\partial q \partial p}^{\Delta}\right]_{\frac{1}{2},\frac{1}{2}}\delta q \delta p \quad . \tag{36}$$

It is apparent from Eqns.(35) and (36) that the term $\frac{1}{2}\frac{\partial^2 u_q}{\partial q^2}\,\delta q^2 + \frac{1}{2}\frac{\partial^2 u_q}{\partial p^2}\,\delta p^2$ has disappeared in the finite difference approximation. The area-weighting is just a bilinear interpolation which introduces an effective viscosity with no physical counterpart.

The velocity of a point inside a mesh cell can then be given by

$$\frac{d\underline{r}}{dt} = \underline{u}_c + \underline{u}_\nu$$

where $\underline{u}_c$ is the correct velocity for an incompressible inviscid fluid, i.e. a solution to

$$\frac{\partial \underline{u}_c}{\partial t} + \underline{u}_c \cdot \nabla \underline{u}_c = -\frac{1}{\rho} \nabla p \ .$$

The velocity $\underline{u}_M = \underline{u}_c + \underline{u}_\nu$ is, however, a solution to

$$\frac{\partial \underline{u}_M}{\partial t} + \underline{u}_M \cdot \nabla \underline{u}_M = -\frac{1}{\rho} \nabla p - \nabla \cdot (\nu_M \nabla \underline{u}_M)$$

with ν_M being the kinematic viscosity $(\frac{\mu}{\rho})$.

The velocity $\underline{u}_\nu$ caused by area-weighting can be calculated assuming again that the correct velocity $\underline{u}_c$ is given by Eq.(33).

We expand the coefficients of the terms in Eqns.(33) and (34). This gives for the q component for mode (r,s) taking terms of second order

$$u_\nu = \left[\tfrac{1}{2} r^2 \delta q(\delta q - 1) + \tfrac{1}{2} s^2 \delta p(\delta p - 1) \right] \cos rq_o \cos sp_o \qquad (37)$$

such that $$u_\nu = \xi \, u_c(q_o \ , \ p_o) \ .$$

The coefficients for sin cos, sin sin, cos sin result in higher order terms. The coefficient of u_ν represents a non-physical viscosity that depends on the position $(\delta q, \delta p)$ within a mesh cell as well as on the mode number (r, s). Since this non-physical viscosity depends on (q, p), the velocity $\underline{u}_M$ does not satisfy Eq.(1). The interpolation used to evaluate $\underline{u}_M$ will thus introduce a non-physical compression of the fluid. The point vortices therefore experience a compressible flow field which will cause them to cluster.

We notice that if $\delta q = 0$ or 1 or $\delta p = 0$ or 1 then the corresponding dependence of r or s respectively correctly vanishes. From Eq.(37) we find

$$\xi = \tfrac{1}{2} r^2 \delta q(\delta q - 1) + \tfrac{1}{2} s^2 \delta p(\delta p - 1) \ ,$$

so that $\xi \leqslant 0$ for all r, s, δq, δp. We also notice the quadratic dependence of the mode numbers ℓ, k. For a given mode ξ_{max} occurs for $\delta q = \delta p = \tfrac{1}{2}$.

We can then roughly state that there is little interference from the interpolation on the long wavelength modes (r, s small), whereas the amplitudes of the short wavelength modes will be diminished. In Fig.1 we assume that p is kept constant and plot u_c and u_ν as functions of q_o and δq

for a long and a short wavelength mode. The maximum amplitude of u_ν is for a given mode $\frac{1}{8} r^2$.

We notice how the short wavelength mode is virtually reduced to zero over the length of a mesh cell.

d) Area-weighting of vorticity

In the approximation (17) f is made up of area contributions as indicated. Analytically we regard a point vortex as described by a Dirac Delta function. Hence the contribution from the point $(q,p) = (q_o+\delta q,\ p_o+\delta p)$ is

$$f = \delta(q-q_o-\delta q)\ \delta(p-p_o-\delta p) \quad .$$

This function can be Fourier analysed and written as

$$f = \frac{2}{N_q}\frac{2}{N_p} \sum_\ell \sum_k a_{\ell k} \cos rq \ \cos sp \tag{38}$$

where we have chosen a cosine expansion in both directions. The coefficient $a_{\ell k}$ is

$$a_{\ell k} = \int_0^{N_q} \int_0^{N_p} f \cos rq \cos sp \, dp \, dq = \frac{1}{rs} \cos r(q_o+\delta q) \cos s(p_o+\delta p) \quad . \tag{39}$$

The area-weighting method credits to the surrounding points amounts A_n given by Eq.(21). Each contribution can be expressed by Eq.(38) but with a coefficient $a_{\ell k}$ obtained from (39) by setting $(\delta q,\delta p) = (0,0)$, $(0,1)$ and $(1,1)$ respectively. The procedure is therefore quite analogous to the one before and the difference between f^Δ and f for mode (r,s) is then to second order

$$\delta f = f^\Delta - f = \tfrac{1}{2} \frac{1}{r} \frac{1}{s} \left[r^2 \delta q(\delta q-1) + s^2 \delta p(\delta p-1) \right] \cos rq \cos sp \quad . \tag{40}$$

The question of interest is now: how many modes in the expansion (38) are required to produce f^Δ ? Or conversely: how many modes in the expansion of f^Δ differ from those of (38) by an amount which is less than a given Δ ? We compare Eqns.(33) and (34)

approximation	analytic
$(1 - \delta q + \delta q \cos r)^D$	$(\cos(r\delta q))^D$
$(\delta q \sin r)^D$	$(\sin(r\delta q))^D$

where D is the dimension of the system.

We form the difference Δ^r between the upper two terms and let D=1 for

simplicity,

$$\Delta^r = \delta q \cos r + 1 - \delta q - \cos(r\delta q) = \sum_n \frac{r^{2n}}{(2n)!} (-1)^n \left[\delta q - \delta q^{2n}\right] . \tag{41}$$

As an example we can ask how many modes are reproduced to within 5% if N is say 64 as in VORTEX.

The expansion (41) becomes

$$\Delta_1^r = -\tfrac{1}{2} \frac{\pi^{2\ell 2}}{64^2} \left[\delta q - \delta q^2\right]$$

$$\Delta_2^r = \frac{1}{24} \frac{\pi^4 \ell^4}{64^4} \left[\delta q - \delta q^4\right] \quad . \tag{42}$$

We notice that $\Delta_2^r \ll (\Delta_1^r)^2$. If we roughly set $\Delta_1^r = 0.05$ then $\Delta_2^r \leqslant 0.0005$. So (42) gives for $\delta q = \tfrac{1}{2}$

$$\ell = \sqrt{\frac{8.64^2 \Delta_1^r}{\pi^2}} \qquad \underline{\ell = 12} \quad ,$$

i.e. the 12 first modes deviate less than 5% from their correct values.

X. FLOW PROPERTIES OF TEST MODEL

Consider a system in which $f = f_o$ inside a circle of radius R_o and zero elsewhere (Fig.2). The stream function resulting from this distribution is a solution to Poisson's equation (5) which in the Hamiltonian coordinates

$$q = \tfrac{1}{2} r^2 \quad , \quad p = \theta \tag{43}$$

becomes

$$\frac{\partial}{\partial q} \left(q \frac{\partial H}{\partial q}\right) + \frac{1}{4q} \frac{\partial^2 H}{\partial p^2} = -\tfrac{1}{2} f \quad . \tag{44}$$

As solution we choose

$$H_1 = -\tfrac{1}{2} f_o (q - q_o) \quad \text{for} \quad q \leqslant q_o$$

and

$$H_2 = -\tfrac{1}{2} f_o \, q_o \log \frac{q}{q_o} \quad \text{for} \quad q \geqslant q_o$$

such that $\frac{\partial H}{\partial q}$ is continuous at the interface $q_o = \tfrac{1}{2} R_o^2$.

Since $f = f_o$ for $0 \leqslant H \leqslant \tfrac{1}{2} f_o q_o$ and $f = 0$ for $H \leqslant 0$ we have a system in equilibrium (12). The system is often referred to as Rankine's combined vortex [11,12]. The metrical coefficients corresponding to q, p given by (43) are

$$h_q = \frac{1}{\sqrt{2q}} \qquad h_p = \sqrt{2q} \ .$$

The velocities u_r, u_θ then become in view of (3)

$$u_r = \frac{1}{h_p}\frac{\partial H}{\partial p} = 0 \tag{45}$$

$$u_\theta = -\frac{1}{h_q}\frac{\partial H}{\partial q} = \tfrac{1}{2} f_o \sqrt{2q} \quad \text{for} \quad 0 \leqslant q \leqslant q_o$$

and

$$u_\theta = \tfrac{1}{2} f_o \frac{2q_o}{\sqrt{2q}} \quad \text{for} \quad q_o \geqslant q \ . \tag{46}$$

Although the f-distribution is discontinuous at $q=q_o$ other quantities like velocity and pressure are continuous functions (Fig.2). The system is an analytic approximation to a motion that is often encountered in real flows. However, viscosity present in the latter will smooth out the f distribution, vorticity will dissipate since $\frac{df}{dt} = \nu^2 \Delta^2 f$ and the vortex will decay exponentially such that in the limit $t \to \infty$ the flow is fully irrotational ($f \approx 0$) [13]. As we neglect viscosity in our study of hydrodynamics we define equilibria as flows obeying Eq.(12).

We can communicate a slight irrotational disturbance, δH, to the system described above such that an oscillating disturbance will cause a stable azimuthal corrugation to travel around the interface q_o with an angular velocity

$$\omega/m = \tfrac{1}{2} f_o \frac{m-1}{m} \tag{47}$$

$$\text{if} \qquad \delta H \sim q^{m/2} \, e^{imp} \ . \tag{48}$$

The equilibrium state of Rankine's combined vortex is linearly stable which is important for our experimental measurements.

XI. THE SET-UP FOR NUMERICAL SIMULATION

To attain a circular region of constant $f=f_o$ we distribute point vortices as shown in Fig.3. On J rings of radii $r_j = jd$, $j = 1,J$ we place point vortices at angles $\theta_{ij} = i \frac{2\pi}{jM}$, $i = 1, jM$. This distribution credits a constant area $\pi d^2 \frac{2J}{(J+1)M}$ to each point vortex.

In the experiments we set $d = 0.3$, $J = 24$, $M = 10$. The total number of particles is 3,000 plus 2 particles in the centre. The area is 163 and the period of rotation is $T_o = \frac{4\pi}{f_o} = 0.682$. We have chosen a value of Δt which is $\frac{16}{3002}$ such that the approximate number of timesteps for one rotation is 128. The maximum velocity occurring at $r = R_o$ is $V_{max} = \tfrac{1}{2} f_o R_o = 66.4$ so that the Courant-Friedrichs-Lewy condition is satisfied ($V_{max} \, \Delta t = 0.35$).

An arrangement similar to the one described has been studied by Morikawa and Swenson [14]. Their study extends to N point vortices, geostrophic or logarithmic, distributed on a circle. The stability analysis of this system is already quite complex as N varies from 2 to 10. With 24 rings present in our experiment we shall make no attempt to analyse the stability. If, however, we simplify the f distribution to be a series of δ-functions $\delta(r-r_j)$ a stability analysis is feasible and the result will be published elsewhere.

In the first series of experiments we place the vortex made up of particles in the centre of a square mesh and normally restrict H to be a constant (0) along the perimeter of the square. The simulation is run for about 1,000 timesteps. Ideally all jM point vortices on ring j should remain on this ring. To see whether this is the case we define the radius function for ring j as

$$r_j(\theta) = \left| \underline{r}_n - \underline{r}_g \right| \tag{49}$$

where $\underline{r}_g$ is the fixed centre of gravity of the jM points on ring j :

$$\underline{r}_g = \frac{1}{jM} \sum_{n=1}^{jM} \underline{r}_n .$$

The radius function can be represented by a finite Fourier series

$$r_j(\theta) = \sum_{m=1}^{L} a_m \, e^{im\theta} \tag{50}$$

where a_m is complex. Evidently $a_o = a_1 = 0$. Since at $t=0$ $a_m = 0$ for all m any development of an azimuthal mode will represent effects that are due to the finite difference formulation or the arrangement of points as explained above.

Analysis of the positions $\underline{r}_i$, i = 1, jM provides us with a_m (m=1,16) as well as the perimeter and area enclosed by the curve they define. The last two quantities are conserved in all experiments to within the level of rounding off errors. In order to assign the anomalies detected to any one of the difference approximations we carry out a number of experiments which are all like Experiment 1 apart from what is outlined below.

Experiment 1: Standard experiment on the vortex as described above.

Experiment 2: Along the square boundary H becomes a function of the distance from the centre of the vortex.

Experiment 3: Δt is varied.

Experiment 4: A single ring of radius $R_d = 6.0$ is moved in a time independent velocity field inherited from Experiment 1.

Experiment 5: As 4 but with $R_d = \frac{7.2^2}{6.0}$.

Experiment 6: As 4 but with $R_d = R_o = 7.2$.

Experiment 7: Test of area weighting method for analytic velocity field.

XII. RESULTS OF THE NUMERICAL EXPERIMENTS

The standard Experiment 1 exhibits an anomalous instability at $r = R_o$ accounted for by a growth with time of the azimuthal modes a_4, a_8, a_{12} as shown in Fig.4. All other modes remain at the level of truncation errors. In order to assign this anomaly to any one of the effects mentioned earlier in this paper we performed the Experiments 2-7 guided by the principle of elimination.

A study of Experiment 1 reveals a deviation in the azimuthal velocity profile as indicated qualitatively in Fig.5. First we look at the effect from using a square boundary since this seems most likely to cause the anomaly. The amplitudes b_4, b_8 ... of the potential $\tilde{H}_{sq}$ (Eq.24) are linearly related [11,12] by

$$a_m = \frac{2m}{f_o} b_m .$$

With our data $a_4 \approx 10^{-5}$. Because of the vector integration technique [9] the accuracy on a position is given by 18 bits or 10^{-5} (in cell length units). We can, therefore, expect the influence of a square boundary to be negligible and indeed Experiment 2 verifies this since a_4 develops in the same way as in Experiment 1. We might now expect that the time integration method could cause the anomalous behaviour in the face of the instability described in Section VIII.

We have however devised a method [8] of preventing the 2 sets of coordinates from getting out of step. The method can be applied at a variable frequency during the time integration and whether used at any frequency or not the development of a_4, a_8 is still present (Experiment 3).

In Experiments 4, 5 and 6 we eliminate all calculations except for the time integration and the area-weighting of velocities (Eq.21). It is now found that inside the vortex the azimuthal modes oscillate with their eigen-

frequencies given by Eq.(47) without growing in time as shown in Fig.6. On the edge and outside the vortex we get the same growth as in Experiments 1-3.

One might have been tempted to attribute the results given above to the leapfrog scheme, since we have shown in Section VIII that this is unstable for irrotational flows, and the outermost ring of the vortex is partly moving irrotationally. However, the area-weighting method can equally well contribute to the results of Experiments 4, 5 and 6. As noticed earlier the area-weighting is a linear interpolation and is thus an exact method when dealing with a flow where u varies linearly as it does inside the vortex. In Experiment 7 we move a particle in a velocity field which is exactly represented at all mesh points. To find the particle velocity we use the formula for area-weighting (Eq.21), and as a trivial test of the method we find an exact representation for a flow described by a linearly varying azimuthal velocity. When moving a particle in a flow field with $u_q = 0$ and $u_p = \frac{1}{2} f_o \frac{2q_o}{\sqrt{2q}}$ (Eq.46) it is found that the area-weighting pushes a particle off the circle it should remain on. The radial velocity component that is introduced by the interpolation will change the radius of the particle orbit by an amount up to 1% during half a rotation period. This is roughly equal to the amplitude of a_4 by that time. Moreover, Experiment 7 confirms the necessity of preventing the two sets of positions from getting out of step as indeed they should in an irrotational motion. The reason why the m=4, 8, 12 .... modes are enhanced is not as we thought initially the introduction of a square boundary. The circular geometry interacts with the square mesh to produce a four-fold symmetry so that only modes with this symmetry can be present. The growth of these modes is caused by the area-weighting and one way to remove this anomaly would be to adopt a higher order interpolation scheme for evaluating the particle velocity. It would be interesting to see whether a change in the structure of the mesh (hexagonal, triagonal etc.) would improve on the accuracy rather than employing more mesh points in the interpolation.

XIII. ADVANTAGES AND DEFICIENCIES OF PARTICLE APPROACH

Two questions that inevitably arise from the foregoing discussions are: How useful is the particle model for a further study of hydrodynamics? And how does it compare with other numerical techniques?

The answer to the first question is based on our experience from a series of numerical situations on a variety of hydrodynamic problems. The particle model has proved useful and reliable within a time range that naturally

depends on what accuracy is needed and what kind of distribution is required. Good agreement has been achieved between theory and a number of experimental results. For a given flow problem that can be described analytically in the linear regime we can by comparing theory and experiment acquire a quantitative understanding of how the inaccuracies are related to the length of the time integration. In most of the cases that we have encountered the prominent part of the evolution takes place before the accumulation of errors can distort the result. For example, in our study of the interaction between vortices the picture of evolution is almost complete within 3, 4 or 5 periods of rotation of a single vortex, limiting the anomalous growth of azimuthal modes to say 5-6%.

A second advantage of the particle approach is its applicability to simulations of guiding centre plasmas [10], thus extending the versatility of the method.

The most serious deficiency is, however, the effect of using a finite number of particles to describe a continuum (hydrodynamic case). The area-weighting inherent from the particle approach introduces a local compression of the fluid, i.e. particle density, and with this effect present the quality of simulating a waterbag system by a discrete distribution of points is lost. A study of the frequency spectrum of f which in the waterbag case should be a delta-function reveals an undesired relaxation of the initially peaked spectrum.

There seems little doubt about the saving in computer time, if the Roberts, Berk method [5] would be applied instead of our method in the study of waterbag systems. But their method sets a limit on the length of the time integration due to a finite computer core store, since the shredding of contours requires more and more points.

The only alternative to our method seems to be a mesh method like the one used by Fromm and Harlow [3]. Their method is subject to conditions for numerical stability analogous to those outlined in [8] but it causes vorticity to diffuse very quickly. In the history of developing our technique the graphical display of the particle positions seemed an attractive feature. With no comparison between the mesh and particle method available at the time of development we were also attracted by the latter because it became clear how to optimize the equations of motion for particles [9].

CONCLUSION

We have described a particle approach to simulate the motion of a continuous hydrodynamic fluid. We have shown how the numerical scheme like any finite difference form contains certain anomalies. Our test problem has however proved that the approximations we have made will not affect the results seriously over a timescale appropriate for a study of many hydrodynamic flows (see Figs. 7 and 8).

ACKNOWLEDGEMENTS

I am indebted to Dr K V Roberts who has been deeply involved in all phases of this work from its inception and who has carefully read and criticized the manuscript. I would also like to thank Dr G Rowlands and Dr J B Taylor for their helpful comments and discussions.

REFERENCES

1. L ONSAGER, Nuovo Cimento Suppl. VI., 130 (1949).
2. G MORIKAWA, J.of Meteorology, 17 (1960).
3. J E FROMM, F H HARLOW, Phys.Fluids, 6, 975 (1963).
4. F H ABERNATHY, R E KRONAUER, J.Fluid Mech. 13, 1 (1962).
5. K V ROBERTS, H L BERK, Phys.Fluids, 10, 1595 (1967).
6. D C DE PACKH, J.Electronics Control, 13, 417 (1962).
7. R A DORY, J.Nuclear Energy (Pt.C), 6 511 (1964).
8. J P CHRISTIANSEN, Culham Report CLM-R106, HMSO.
9. J P BORIS, K V ROBERTS, J.Comp.Phys. 4. 552 (1969).
10. J B TAYLOR, B MCNAMARA, Phys.Fluids, 14, 1492 (1971)
11. H LAMB, Hydrodynamics, 6th Ed., Cambridge University Press (1932).
12. A B BASSETT, Hydrodynamics Vol.2, Dover Publications Inc. (1961).
13. L TING, C TUNG, Phys.Fluids, 8, 1039 (1965).
14. J P CHRISTIANSEN, R W HOCKNEY, Comp.Phys.Comm. 2, No.3, (1971).
15. R L MORSE, Methods in Computational Physics, Vol.9, Academic Press (1970).
16. G MORIKAWA, E V SWENSON, Phys.Fluids, 14, 1058 (1971).
17. C K BIRDSALL, D FUSS, J.Comp.Phys. 3, 494 (1969).
18. R W HOCKNEY, Methods in Computational Physics, Vol.9, Academic Press (1970)
19. A B LANGDON, J.Comp.Phys. 6, 247 (1970).

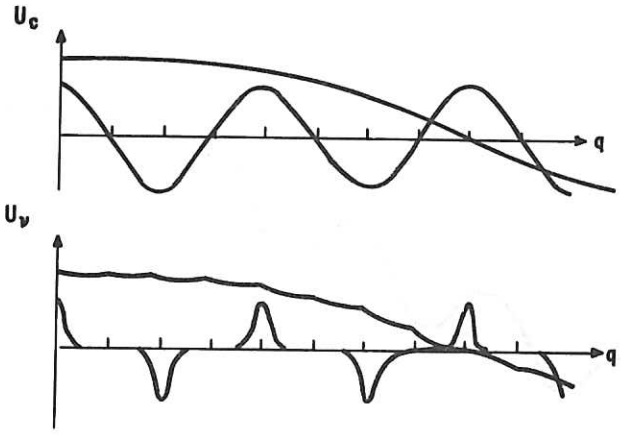

Fig. 1 Effect of CIC interpolation on long and short lengths

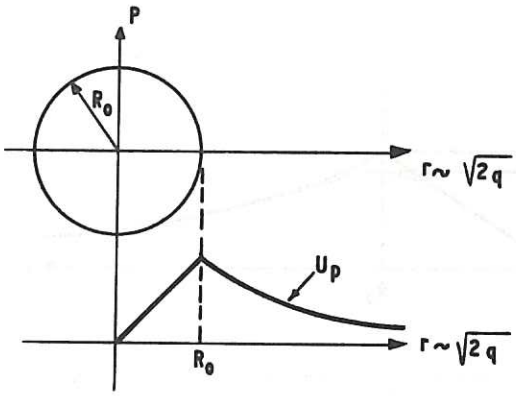

Fig. 2 Rankine's combined vortex as test model

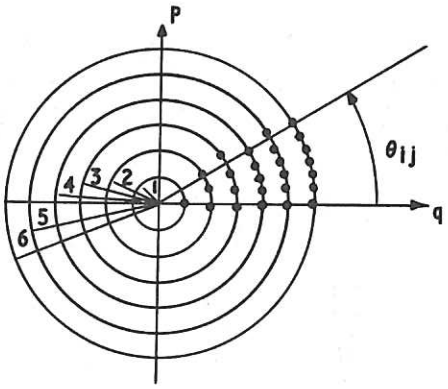

Fig. 3 Point vortices arranged to simulate Rankine's combined vortex

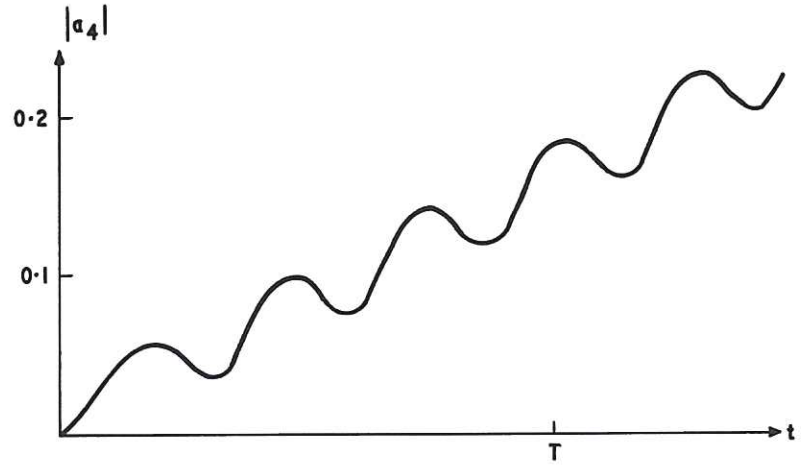

Fig. 4 Amplitude of the m=4 azimuthal mode versus time, measured at r = 7.2

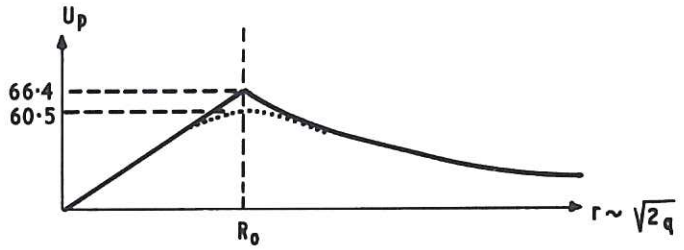

Fig. 5 Azimuthal velocity profile. Dotted line indicates the profile found in the experiment

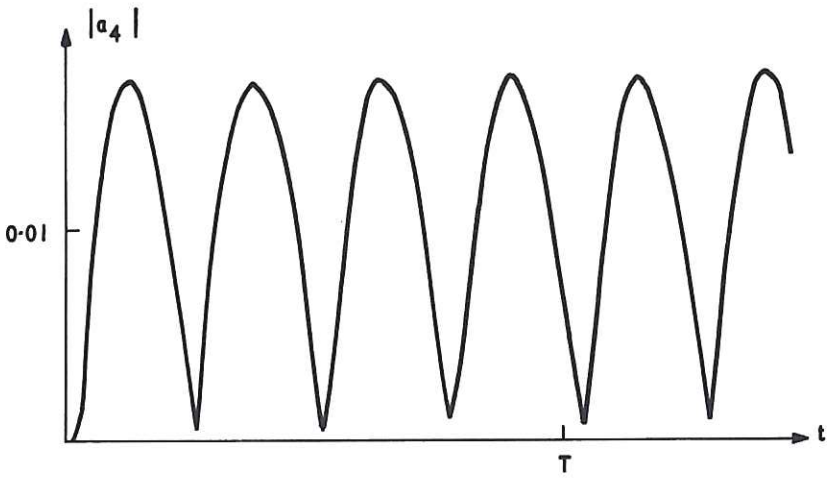

Fig. 6 Amplitude of the m=4 azimuthal versus time, measured at r = 6.0

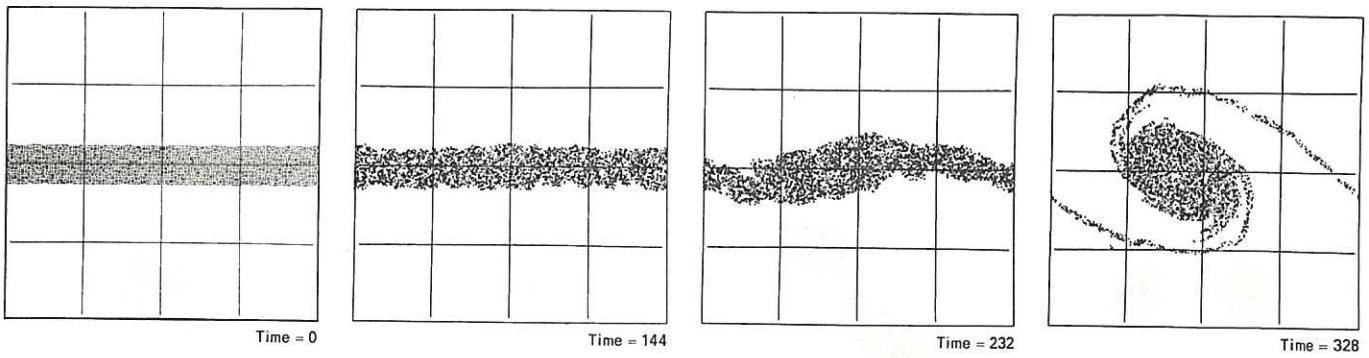

The onset of the Kelvin-Helmholtz instability

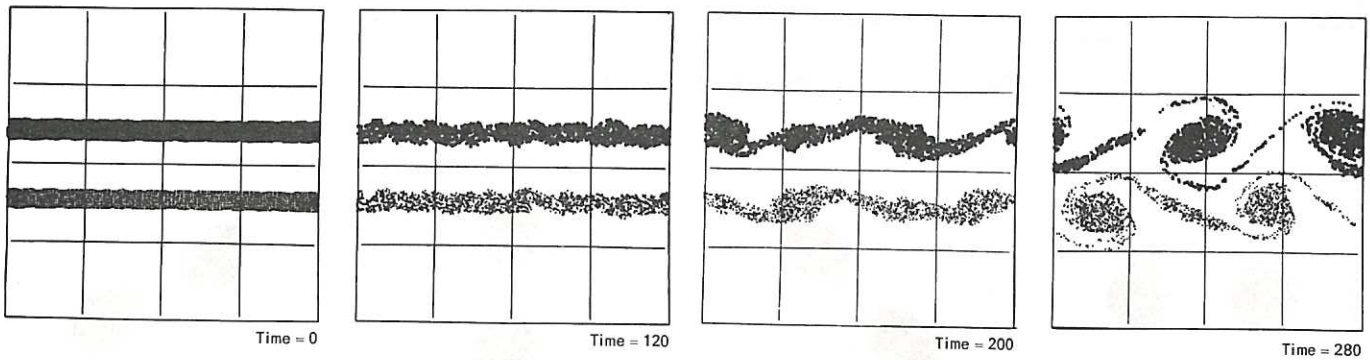

The formation of the von Karman vortex street

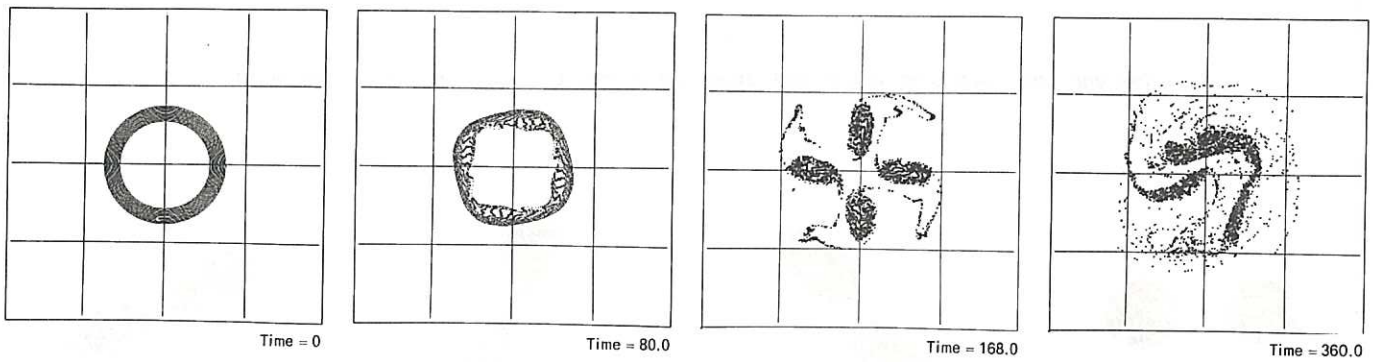

Sheared rotation. Diochotron type instability

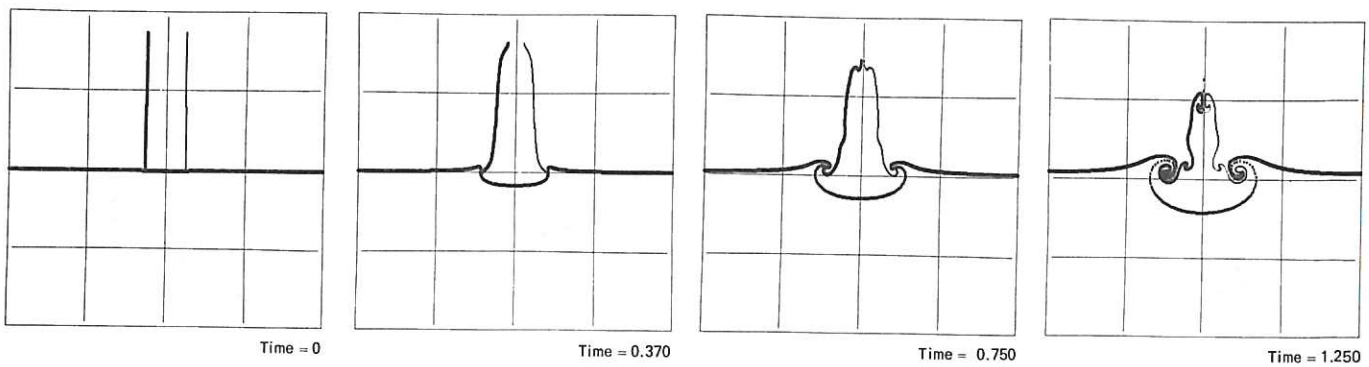

Penetration of a jet. The crinkling up of the edges results in two vortices of opposite polarity

Fig. 7 Flow problems simulated by program VORTEX

CLM - P282

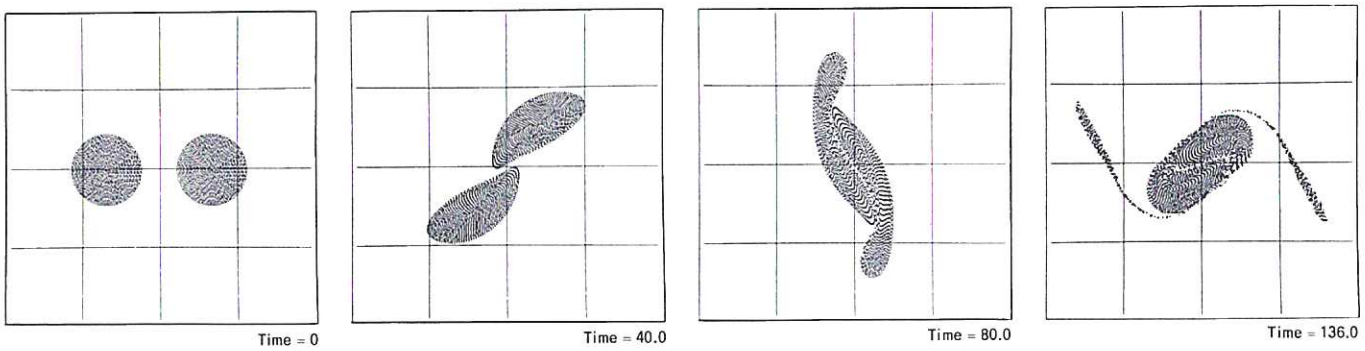

Two vortices coalescing because of sufficient initial proximity

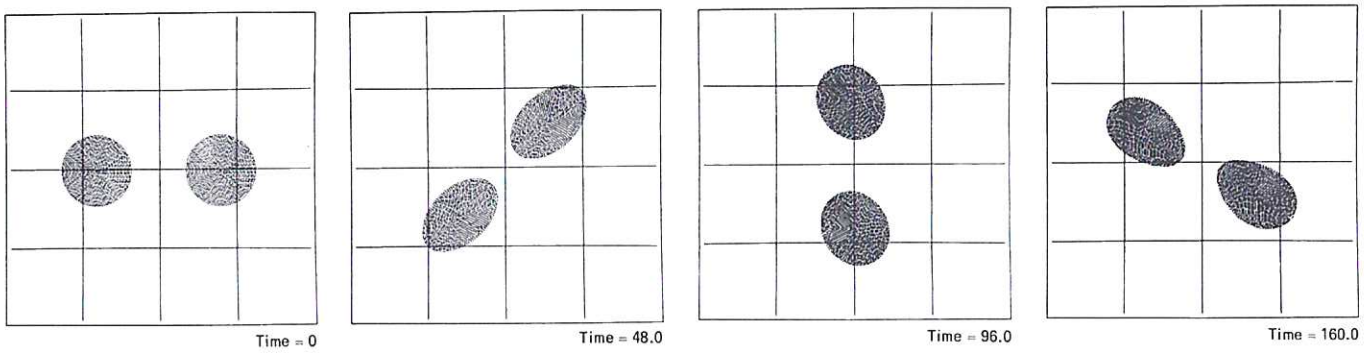

Two vortices precessing around each other. Large amplitude oscillations on their surfaces

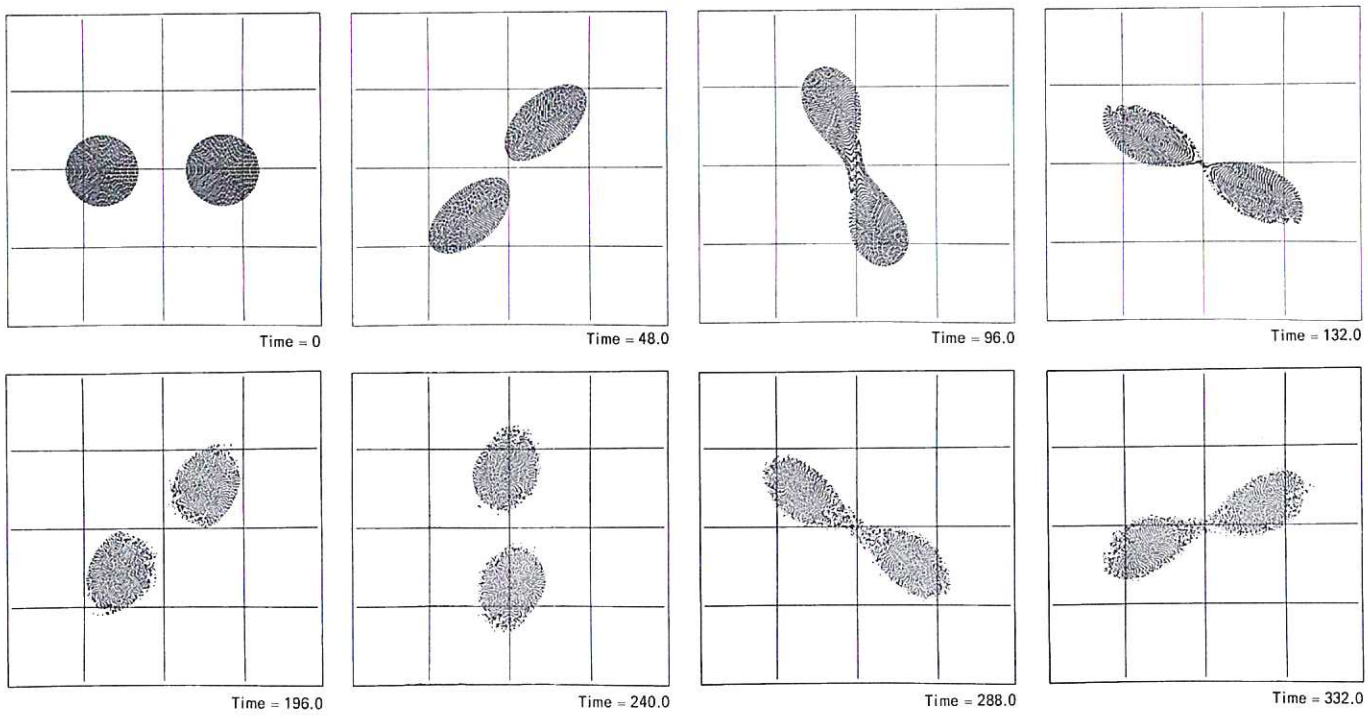

Two vortices with a critical initial proximity. At the approach they exchange vortex fluid

Fig. 8 The elementary interaction between two vortices of the same polarity